

Sublithospheric small-scale convection—A mechanism for collision zone magmatism

L. Kaislaniemi, J. van Hunen, M.B. Allen, and I. Neill

Department of Earth Sciences, Durham University, Science Labs, DH1 3LE Durham, UK

ABSTRACT

We studied the effect of increased water content on the dynamics of the lithosphere-asthenosphere boundary in a postsubduction setting. Results from numerical mantle convection models show that the resultant decrease in mantle viscosity and the peridotite solidus produce small-scale convection at the lithosphere-asthenosphere boundary and magmatism that follows the spatially and temporally scattered style and volumes typical for collision magmatism, such as the late Cenozoic volcanism of the Turkish-Iranian Plateau. An inherent feature in small-scale convection is its chaotic nature that can lead to temporally isolated volcanic centers tens of millions of years after initial continental collision, without evident tectonic cause. We also conclude that water input into the upper mantle during and after subduction under the circum-Mediterranean area and the Tibetan Plateau can account for the observed magmatism in these areas. Only fractions (200–600 ppm) of the water input need to be retained after subduction to induce small-scale convection and magmatism on the scale of those observed from the Turkish-Iranian Plateau.

INTRODUCTION

Compared with subduction-related magmatism, mantle-derived collision zone magmatism is still poorly understood. Suggested explanations include increased radiogenic heat production (England and Thompson, 1984), mantle lithosphere delamination (Bird, 1978), slab break-off (Davies and von Blanckenburg, 1995), edge-driven convection (Missenard and Cadoux, 2012), and compressional melting due to breakdown of hydrous phases in the thickening mantle lithosphere (Allen et al., 2013). We studied the dynamics of the postsubduction syncollisional mantle with the hypothesis that the upper mantle on the overriding plate side has been hydrated, leading to instability of the lithosphere-asthenosphere boundary, sublithospheric small-scale convection (Hernlund et al., 2008), and consequent melting. We compare our model to the volcanic record of the Turkish-Iranian Plateau to explain distinctive features of the volcanism, i.e., scattered centers with no clear temporal or spatial patterns and with varying geochemical signatures (e.g., Pearce et al., 1990; Dilek et al., 2010).

Collision Zone Magmatism of the Turkish-Iranian Plateau

Collision of the Arabian and Eurasian plates began ca. 25–35 Ma with the end of northward oceanic subduction of the Neo-Tethys (see McQuarrie and van Hinsbergen, 2013, and references therein). Collision has continued to the present day, evidenced by the frequent earthquakes in southwest Asia and the current ~15–25 mm/yr northward convergence of Arabia with Eurasia (Vernant et al., 2004). Active crustal thickening and shortening take place at the plateau margins. Following a period of limited Oligocene–Miocene magmatism, there has been an upsurge in magmatic activity across the collision zone in the past few million years (Keskin et al., 1998; Chiu et al., 2013), with widespread if scattered centers focused on the high region with low relief known as the Turkish-Iranian Plateau (Fig. 1).

Collision magmatism of the plateau is highly variable in composition, varying from basaltic to rhyolitic, calc-alkaline to alkaline, arc like to within-plate like (e.g., Pearce et al., 1990; Keskin et al., 1998; Neill et al., 2013). The most voluminous volcanism is in eastern Anatolia, where thicknesses of the volcanic sequences locally exceed 1 km and cover two-thirds of the region, with an average thickness of a few hundred meters (Keskin et al., 1998).

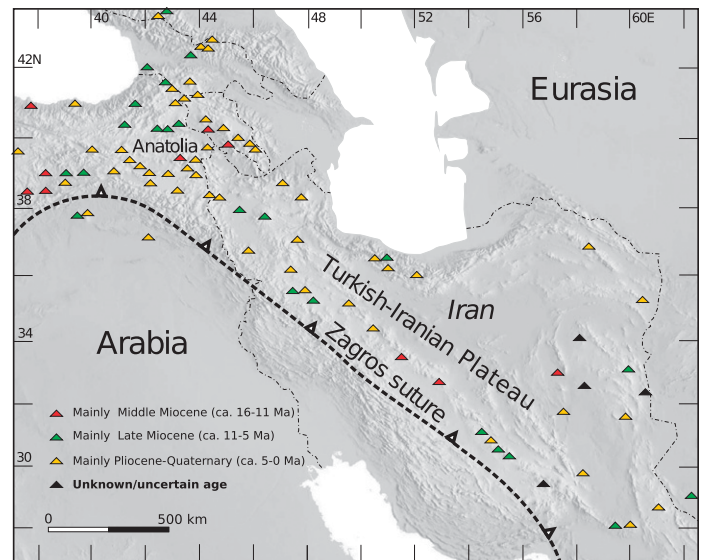


Figure 1. Distribution of Middle Miocene to recent (16–0 Ma) volcanic centers of Turkish-Iranian Plateau; background is topography map (modified after Neill et al., 2013). See the Data Repository (see footnote 1) for numeric values and references for ages.

Trace element characteristics of the least-evolved magmas indicate subduction-modified lithospheric mantle sources (high Th/Yb, La/Nb) with or without an ocean island basalt (OIB)-like asthenospheric component (Pearce et al., 1990; Keskin et al., 1998; Neill et al., 2013). Rarer OIB-like centers with low Th/Yb and La/Nb are also found (Pang et al., 2012). Low-degree melting ($\ll 10\%$) occurred in the spinel stability field or in some cases deeper (>75 km) in the garnet stability field (Pang et al., 2012; Neill et al., 2013). Some more evolved centers show extensive Sr isotope evidence for crustal contamination (Pearce et al., 1990).

The magmatism has been attributed to slab break-off (Keskin, 2003) and/or lithospheric delamination (e.g., Pearce et al., 1990). Seismic studies give support to these ideas, as the lithosphere at a distance from the suture is relatively thin (<100 km in eastern Anatolia and adjacent areas) with low shear wave velocities at 100 km depth (Maggi and Priestley, 2005; Angus et al., 2006). However, low seismic velocities could partly be explained by compositional variation (e.g., high fluid content, partial melts) of the lower lithosphere rather than by its absence (Kaviani et al., 2007). Magmatism also occurs in areas with lithosphere >100 km thick (Allen et al., 2013). The nature of slab break-off or delamination mechanisms is such that they would produce spatially and chronologically correlated patterns of magmatism. The propagation of the slab detachment is expected to produce more or less linear segments of magmatism, close to the trench, with a clear time-space relationship (Davies and von Blanckenburg, 1995; van Hunen and Allen, 2011). The delamination of the lithospheric mantle as one coherent sliver (sensu Bird, 1978) causes the replacement of lithospheric mantle by asthenospheric mantle and consequent melting, propagating in the direction of the delamination and waning as the lithosphere cools down. Such features are not clearly observed on the Turkish-Iranian Plateau (Fig. 1). Essentially singular events like slab break-off and delamination cannot

alone explain magmatism that has a long history and shows no clear patterns in space or in time.

Here we suggest that the irregularity of the long-term syncollisional magmatism can be explained by small-scale sublithospheric convection, effectively a form of repeated and localized lithosphere delamination or dripping (as opposed to one-time regional catastrophic delamination), induced by the viscosity- and solidus-lowering effect of water added to the upper mantle by the precollision subduction, and possibly enhanced by asthenospheric stirring triggered by slab break-off.

WATER IN THE MANTLE

Our model relies on the assumption that the mantle on the overriding plate side was hydrated during subduction and retains some water left from melting of the mantle wedge. We assume mantle water contents of 200–600 wt ppm that lead to viscosity decrease, instability of the lithosphere-asthenosphere boundary, and thus to small-scale convection. The chosen range of water contents exceeds ambient asthenospheric concentrations [i.e., ~120 wt ppm H₂O for mid-oceanic ridge basalt (MORB) source mantle; Dixon et al., 2004], for which no magmatism should be expected. Chosen water contents are still small compared to the amounts causing arc magmatism in active subduction (2500–10000 wt ppm; Dixon et al., 2004) and cannot produce arc-like magmatism.

More than 2000 wt ppm of water can be incorporated into the nominally anhydrous minerals of the mantle peridotite at asthenospheric conditions (Hirschmann et al., 2005). Direct observations from lherzolitic xenoliths have confirmed concentrations of 28–175 wt ppm in the continental lithospheric mantle, and based on these observations the maximum water content of primitive mantle is estimated to be 245 wt ppm for garnet and 290 wt ppm for spinel lherzolite (Bell and Rossman, 1992). The estimated partition coefficients of water led Bell et al. (2004) to conclude that ~100–200 wt ppm of water could be retained in the wedge melting residues above subduction zones.

Distribution of the hydrated mantle after subduction is unclear, but two observations suggest that elevated upper mantle water contents may exist over a large area and persist for significant periods after subduction has ceased. (1) The source regions of the backarc volcanism of active subduction zones show water content values above MORB source region values even as much as 400 km away from the trench (a global compilation of glasses and olivine hosted melt inclusions; Kelley et al., 2006). (2) Hydrous, potassic volcanism with arc affinities for tens of millions of years after active subduction has been observed, thus implying that the mantle can remain hydrated on at least these time scales (e.g., Feldstein and Lange, 1999, and references therein). Wadsleyite, a high-pressure polymorph of olivine, is able to hold as much as 20,000 wt ppm water at the mantle transition zone below subduction zones, and could also be a source of water in the upper mantle (Richard and Iwamori, 2010).

GEODYNAMIC MODELING

We quantify the role of lithospheric dripping on magmatism using geodynamic models for the upper mantle and crust, taking into account the role of increased water content on lithosphere stability and melting. The model comprises an initially 100-km-thick (1350 °C isotherm) lithosphere, which represents the overriding plate after active subduction has ceased. The model domain is homogeneously hydrated with various amounts of water, taken to be left from the previous subduction.

Mantle melting is parameterized using the hydrous peridotite melting model by Katz et al. (2003) that takes into account the solidus lowering effect of water at varying pressure. Water is handled as an incompatible element with bulk distribution coefficient, $D = 0.01$, and is removed with the melt at each time step using a batch melting model. Melt depletion affects the mantle density by making it more buoyant (Schutt and Lesher, 2006).

We take into account the effect of water on mantle rheology (e.g., Hirth and Kohlstedt, 2003). We parameterize the weakening with

$$\eta_{\text{hydrous}} = W\eta_{\text{dry}}, \text{ where } W = 100^{\frac{-X_{\text{H}_2\text{O}}}{X_{\text{H}_2\text{O}}+a}}, \quad (1)$$

where $X_{\text{H}_2\text{O}}$ (wt ppm) is the bulk water content and a (wt ppm) is the water sensitivity parameter controlling how large $X_{\text{H}_2\text{O}}$ needs to be to decrease the viscosity by factor of 10. This parameterization is constrained by experimental results showing that viscosity in hydrous olivine aggregates decreases exponentially with the water fugacity, and that the maximum difference between dry and water saturated viscosities is about two orders of magnitude (Hirth and Kohlstedt, 2003). The water sensitivity parameter captures the effects of multiple physical parameters (value of the exponent, water content and water fugacity relationship, water partitioning between mantle minerals) and their uncertainties, but has a clear physical meaning (rheological sensitivity to water), thus allowing an easier parameter study of the effects of water on the formation of small-scale convection. We use values of 200–500 ppm for a , leading to viscosity weakening of 0.7–1.4 orders of magnitude. The lower boundary is restricted by assuming that ambient mantle water contents should not lead to significant weakening, whereas values of $a > 500$ ppm do not change the results significantly compared to the case of $a = 500$ ppm. The viscosity parameterization leads to minimum effective dry asthenospheric viscosities of 5×10^{19} Pa·s. (For a detailed method description, see the GSA Data Repository¹.)

MODELING RESULTS

Reduced viscosity, due to the elevated water content, increases the vigor of convection, leads to instability of the base of the lithosphere, and so to dripping of the lithosphere into the underlying asthenosphere. There is no significant permanent thinning of the lithosphere. A small-scale convection pattern forms at the lithosphere-asthenosphere boundary (Fig. 2), with convection cell diameters ranging from <100–300 km. This convection makes decompression melting of the asthenosphere possible.

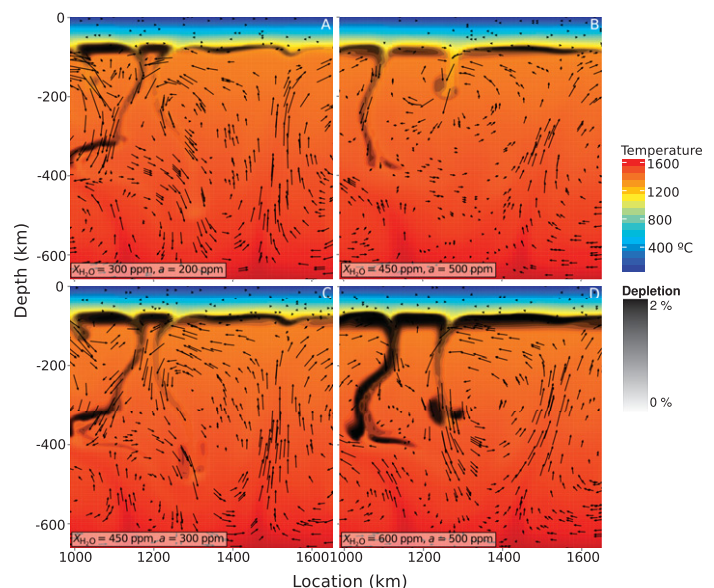


Figure 2. Detailed view of model domain showing temperature, velocity (arrows), and depletion fields at time = 15 Ma with different water sensitivity parameters (a) and water content. Models shown correspond to models circled in Figure 4.

¹GSA Data Repository item 2014110, supplemental information including a detailed method description and references for Figure 1, is available online at www.geosociety.org/pubs/ft2014.htm, or on request from editing@geosociety.org or Documents Secretary, GSA, P.O. Box 9140, Boulder, CO 80301, USA.

The viscosity of the melt-depleted mantle material increases because of the partial removal of the water with the partial melts. Depleted mantle, being more viscous and more buoyant, adheres to the bottom of the lithosphere for a while before being removed by the convection. This can cause the melting in the convection cell to pause. The convection cells migrate laterally, so that the locations of decompression melting also change; the behavior is seemingly random.

Plotting the rate of volcanism against time and location (Fig. 3) shows an irregular pattern, where the volcanic centers are active from less than a couple of million years to tens of millions of years, and can have significant time lags after the start of the postsubduction period. Production rates vary between <20 m/m.y. to hundreds of meters per million years. In all estimates of the volume or production rate of the volcanism in our results, mantle melts are assumed to percolate directly and instantaneously to the surface, forming a volcanic layer with average thickness. In reality, only a certain proportion of the melts produced contribute to the extrusions visible at the surface. The total volume of melt produced for different values of a and X_{H_2O} is shown in Figure 4.

DISCUSSION

The temporal and spatial patterns of magma production (Fig. 3) are irregular but all have dominating spatial wavelengths of ~200 km (fast Fourier transform analysis; see the Data Repository). This corresponds to the typical distances (Fig. 3) between larger volcanic centers in the models. Reactivation time (Fig. 3) of the larger volcanic centers depends on the total viscosity decrease, but generally ranges from 5 to 20 m.y. With lower H_2O dependency of viscosity, the volcanic centers tend to have longer, more diffuse lifespans, whereas higher H_2O dependency produces shorter lifespans with more frequent reactivation (cf. Figs. 3A and 3B).

This irregular pattern of volcanism is the most striking feature common to both our models and the volcanism of the Turkish-Iranian Plateau. The appearance of a volcanic center millions of years after the initial collision can be simply explained by the chaotic nature of the small-scale convection. The heterogeneous chemical signature of the volcanism, a

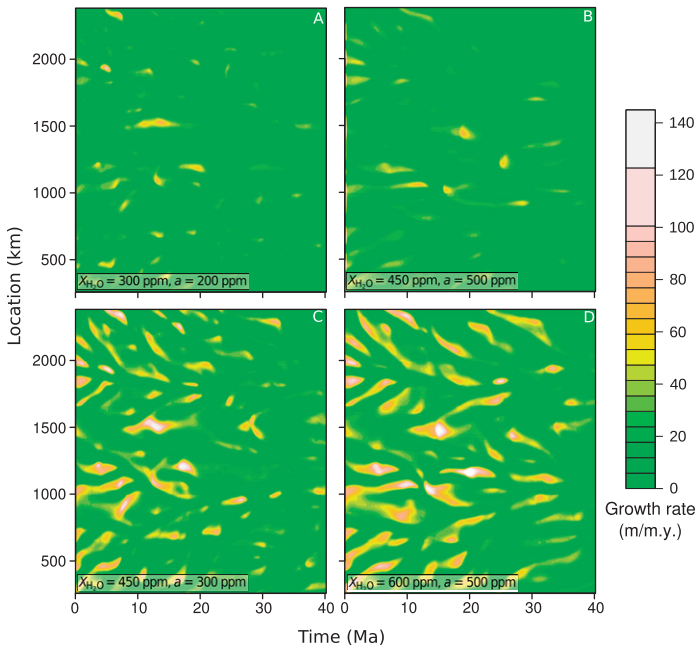


Figure 3. Rate of volcanism (assuming extrusive magmatism only) with different water sensitivity parameters (a) and water content. Magmatism distributed laterally over the model domain (vertical axis) is plotted against time (horizontal axis). Models shown correspond to those in Figure 2 and to models circled in Figure 4.

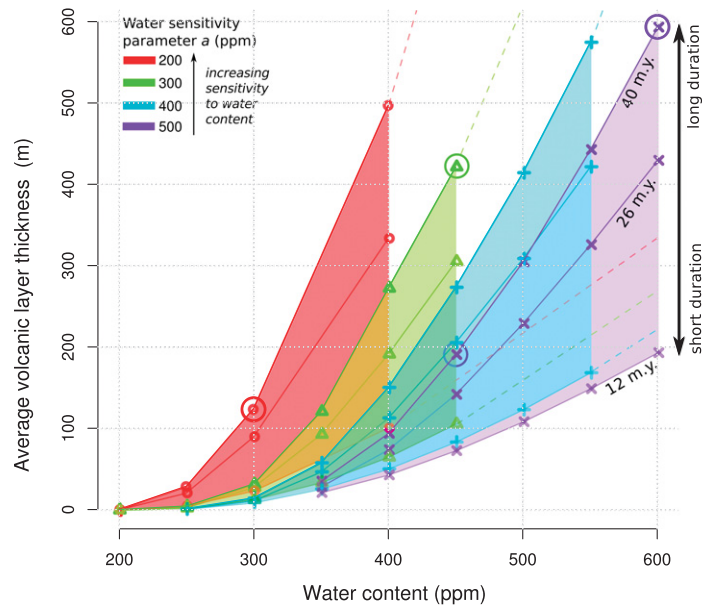


Figure 4. Average thickness of volcanic rocks as function of water sensitivity parameter a , initial amount of water in mantle, and model run duration. Dashed lines show extrapolation to unexplored region of parameter space. Models used in Figures 2 and 3 are circled.

result of variable asthenospheric and lithospheric mantle contributions to melting, can be explained by the small-scale convection effectively mixing lithosphere with asthenosphere near the spinel-garnet transition zone. In addition to the decompression melting, convection advectively heats the lithosphere, and can aid the compressional melting of hydrous phases of the lithosphere as it is being dripped down to the asthenosphere.

The most voluminous volcanism of the plateau, in eastern Anatolia, covers two-thirds of the area and averages perhaps a few hundred meters in thickness (e.g., Keskin et al., 1998). These amounts can be reproduced with many combinations of water content and water sensitivity (Fig. 4), even if intrusive magmatism is significant in amount, showing that small-scale convection is a viable mechanism for the volcanism, regardless of the uncertainties in water content and parameter a .

The thinning of the thermal lithosphere is too minor to produce significant uplift. It is more important that small-scale convection can lead to localized thinning of the lithosphere, thus creating favorable conditions for the start of complete (catastrophic) mantle delamination, as described by Morency and Doin (2004). Nevertheless, our results show that no whole mantle delamination is required to produce voluminous collision zone volcanism. An extended period of magmatism (tens of millions of years) after the onset of continental collision is an inherent feature of the water-induced instability of the lithosphere-asthenosphere boundary and sublithospheric small-scale convection, and requires no other explanation than the input of water to the lithospheric and asthenospheric mantle during previous subduction. Small-scale convection could be enhanced by slab break-off or wholesale lithospheric mantle delamination, but neither of these is prerequisite for small-scale convection and the resultant magmatism.

The general mechanism of water weakening and volcanism produced by small-scale convection could also be applied at a larger scale to the anorogenic igneous activity of the circum-Mediterranean region (Lustrino and Wilson, 2007), where large areas of mantle transition zone might have been hydrated by the Mediterranean subduction zones (Nolet and Zielhuis, 1994). We furthermore suggest applications of this model for the Tibetan Plateau, where localized magmatism has been a persistent feature of the India-Eurasia collision zone (Chung et al., 2005). More generally, occurrence of long-lasting magmatism without evident

tectonic cause, sedimentation, or faulting can be explained by the activation of the most basal lithosphere whenever enough water is present, without the need to involve different theories for the cause of each volcanic center separately.

ACKNOWLEDGMENTS

We thank Nancy McMillan and an anonymous reviewer for useful and constructive reviews. This work has been supported by the European Union FP7 Marie Curie Initial Training Network Topomod, contract 264517 (Kaislaniemi); van Hunen acknowledges funding from the European Research Council (ERC Starting Grant 279828). Allen and Neill are supported by the Natural Environment Research Council standard grant (NE/H021620/1) Orogenic Plateau Magmatism.

REFERENCES CITED

- Allen, M.B., Kheirkhah, M., Neill, I., Emami, M.H., and McLeod, C.L., 2013, Generation of arc and within-plate chemical signatures in collision zone magmatism: Quaternary lavas from Kurdistan Province, Iran: *Journal of Petrology*, v. 54, p. 887–911, doi:10.1093/petrology/egs090.
- Angus, D.A., Wilson, D.C., Sandvol, E., and Ni, J.F., 2006, Lithospheric structure of the Arabian and Eurasian collision zone in eastern Turkey from S-wave receiver functions: *Geophysical Journal International*, v. 166, p. 1335–1346, doi:10.1111/j.1365-246X.2006.03070.x.
- Bell, D.R., and Rossman, G.R., 1992, Water in Earth's mantle: The role of nominally anhydrous minerals: *Science*, v. 255, p. 1391–1397, doi:10.1126/science.255.5050.1391.
- Bell, D.R., Rossman, G.R., and Moore, R.O., 2004, Abundance and partitioning of OH in a high-pressure magmatic system: Megacrysts from the Monastery Kimberlite, South Africa: *Journal of Petrology*, v. 45, p. 1539–1564, doi:10.1093/petrology/egh015.
- Bird, P., 1978, Initiation of intracontinental subduction in the Himalaya: *Journal of Geophysical Research*, v. 83, no. B10, p. 4975–4987, doi:10.1029/JB083iB10p04975.
- Chiu, H.-Y., Chung, S.-L., Zarrinkoub, M.H., Mohammadi, S.S., Khatib, M.M., and Iizuka, Y., 2013, Zircon U-Pb age constraints from Iran on the magmatic evolution related to Neotethyan subduction and Zagros orogeny: *Lithos*, v. 162–163, p. 70–87, doi:10.1016/j.lithos.2013.01.006.
- Chung, S.-L., Chu, M.-F., Zhang, Y., Xie, Y., Lo, C.-H., Lee, T.-Y., Lan, C.-Y., Li, X., Zhang, Q., and Wang, Y., 2005, Tibetan tectonic evolution inferred from spatial and temporal variations in post-collisional magmatism: *Earth-Science Reviews*, v. 68, p. 173–196, doi:10.1016/j.earscirev.2004.05.001.
- Davies, J.H., and von Blanckenburg, F., 1995, Slab breakoff: A model of lithosphere detachment and its test in the magmatism and deformation of collisional orogens: *Earth and Planetary Science Letters*, v. 129, p. 85–102, doi:10.1016/0012-821X(94)00237-S.
- Dilek, Y., Imamverdiyev, N., and Altunkaynak, Ş., 2010, Geochemistry and tectonics of Cenozoic volcanism in the Lesser Caucasus (Azerbaijan) and the peri-Arabian region: Collision-induced mantle dynamics and its magmatic fingerprint: *International Geology Review*, v. 52, p. 536–578, doi:10.1080/00206810903360422.
- Dixon, J.E., Dixon, T.H., Bell, D.R., and Malservisi, R., 2004, Lateral variation in upper mantle viscosity: Role of water: *Earth and Planetary Science Letters*, v. 222, p. 451–467, doi:10.1016/j.epsl.2004.03.022.
- England, P.C., and Thompson, A.B., 1984, Pressure-temperature-time paths of regional metamorphism I. Heat transfer during the evolution of regions of thickened continental crust: *Journal of Petrology*, v. 25, p. 894–928, doi:10.1093/petrology/25.4.894.
- Feldstein, S.N., and Lange, R.A., 1999, Pliocene potassic magmas from the Kings River region, Sierra Nevada, California: Evidence for melting of a subduction-modified mantle: *Journal of Petrology*, v. 40, p. 1301–1320, doi:10.1093/petroj/40.8.1301.
- Hernlund, J.W., Tackley, P.J., and Stevenson, D.J., 2008, Buoyant melting instabilities beneath extending lithosphere: I. Numerical models: *Journal of Geophysical Research*, v. 113, B04405, doi:10.1029/2006JB004862.
- Hirschmann, M.M., Aubaud, C., and Withers, A.C., 2005, Storage capacity of H₂O in nominally anhydrous minerals in the upper mantle: *Earth and Planetary Science Letters*, v. 236, p. 167–181, doi:10.1016/j.epsl.2005.04.022.
- Hirth, G., and Kohlstedt, D., 2003, Rheology of the upper mantle and the mantle wedge: A view from the experimentalists, in Eiler, J., ed., *Inside the subduction factory*: American Geophysical Union Geophysical Monograph 183, p. 83–105, doi:10.1029/138GM06.
- Katz, R.F., Spiegelman, M., and Langmuir, C.H., 2003, A new parameterization of hydrous mantle melting: *Geochemistry Geophysics Geosystems*, v. 4, 1073, doi:10.1029/2002GC000433.
- Kavianii, A., Paul, A., Bourova, E., Hatzfeld, D., Pedersen, H., and Mokhtari, M., 2007, A strong seismic velocity contrast in the shallow mantle across the Zagros collision zone (Iran): *Geophysical Journal International*, v. 171, p. 399–410, doi:10.1111/j.1365-246X.2007.03535.x.
- Kelley, K.A., Plank, T., Grove, T.L., Stolper, E.M., Newman, S., and Hauri, E., 2006, Mantle melting as a function of water content beneath back-arc basins: *Journal of Geophysical Research*, v. 111, no. B9, B09208, doi:10.1029/2005JB003732.
- Keskin, M., 2003, Magma generation by slab steepening and breakoff beneath a subduction-accretion complex: An alternative model for collision-related volcanism in Eastern Anatolia, Turkey: *Geophysical Research Letters*, v. 30, p. 7–10, doi:10.1029/2003GL018019.
- Keskin, M., Pearce, J.A., and Mitchell, J.G., 1998, Volcano-stratigraphy and geochemistry of collision-related volcanism on the Erzurum-Kars Plateau, northeastern Turkey: *Journal of Volcanology and Geothermal Research*, v. 85, p. 355–404, doi:10.1016/S0377-0273(98)00063-8.
- Lustrino, M., and Wilson, M., 2007, The circum-Mediterranean anorogenic Cenozoic igneous province: *Earth-Science Reviews*, v. 81, p. 1–65, doi:10.1016/j.earscirev.2006.09.002.
- Maggi, A., and Priestley, K., 2005, Surface waveform tomography of the Turkish-Iranian plateau: *Geophysical Journal International*, v. 160, p. 1068–1080, doi:10.1111/j.1365-246X.2005.02505.x.
- McQuarrie, N., and van Hinsbergen, D.J.J., 2013, Retrodeforming the Arabia-Eurasia collision zone: Age of collision versus magnitude of continental subduction: *Geology*, v. 41, p. 315–318, doi:10.1130/G33591.1.
- Missenard, Y., and Cadoux, A., 2012, Can Moroccan Atlas lithospheric thinning and volcanism be induced by edge-driven convection?: *Terra Nova*, v. 24, p. 27–33, doi:10.1111/j.1365-3121.2011.01033.x.
- Morency, C., and Doin, M.-P., 2004, Numerical simulations of the mantle lithosphere delamination: *Journal of Geophysical Research*, v. 109, B03410, doi:10.1029/2003JB002414.
- Neill, I., Meliksetian, K., Allen, M.B., Navarsardyan, G., and Karapetyan, S., 2013, Pliocene–Quaternary volcanic rocks of NW Armenia: Magmatism and lithospheric dynamics within an active orogenic plateau: *Lithos*, v. 180–181, p. 200–215, doi:10.1016/j.lithos.2013.05.005.
- Nolet, G., and Zielhuis, A., 1994, Low S velocities under the Tornquist-Teisseyre zone: Evidence for water injection into the transition zone by subduction: *Journal of Geophysical Research*, v. 99, p. 15813–15820, doi:10.1029/94JB00083.
- Pang, K.-N., Chung, S.-L., Zarrinkoub, M.H., Mohammadi, S.S., Yang, H.-M., Chu, C.-H., Lee, H.-Y., and Lo, C.-H., 2012, Age, geochemical characteristics and petrogenesis of late Cenozoic intraplate alkali basalts in the Lut-Sistan region, eastern Iran: *Chemical Geology*, v. 306–307, p. 40–53, doi:10.1016/j.chemgeo.2012.02.020.
- Pearce, J.A., Bender, J.F., Delong, S.E., Kidd, W.S.F., Low, P.J., Guner, Y., Saroglu, F., Yılmaz, Y., Moor bath, S., and Mitchell, J.G., 1990, Genesis of collision volcanism in Eastern Anatolia, Turkey: *Journal of Volcanology and Geothermal Research*, v. 44, p. 189–229, doi:10.1016/0377-0273(90)90018-B.
- Richard, G.C., and Iwamori, H., 2010, Stagnant slab, wet plumes and Cenozoic volcanism in East Asia: *Physics of the Earth and Planetary Interiors*, v. 183, p. 280–287, doi:10.1016/j.pepi.2010.02.009.
- Schutt, D.L., and Leshner, C.E., 2006, Effects of melt depletion on the density and seismic velocity of garnet and spinel lherzolite: *Journal of Geophysical Research*, v. 111, p. 1–24, doi:10.1029/2003JB002950.
- van Hunen, J., and Allen, M.B., 2011, Continental collision and slab break-off: A comparison of 3-D numerical models with observations: *Earth and Planetary Science Letters*, v. 302, p. 27–37, doi:10.1016/j.epsl.2010.11.035.
- Vernant, P., Nilforoushan, F., Hatzfeld, D., Abbassi, M.R., Vigny, C., Masson, F., Nankali, H., Martinod, J., Ashtiani, A., Bayer, R., Tavakoli, F., and Chéry, J., 2004, Present-day crustal deformation and plate kinematics in the Middle East constrained by GPS measurements in Iran and northern Oman: *Geophysical Journal International*, v. 157, p. 381–398, doi:10.1111/j.1365-246X.2004.02222.x.

Manuscript received 11 October 2013

Revised manuscript received 21 December 2013

Manuscript accepted 10 January 2014

Printed in USA